Direct and integration methods of parameter estimation in groundwater transport systems

Jiannan Xiang and Derek Elsworth

Department of Mineral Engineering, The Pennsylvania State University, University Park, PA, USA

Two finite element based methods are developed to identify the spatial distribution of parameters that characterize contaminant transport in two-dimensional irrotational potential flow in the regions over which a concentration front has passed. The required input data are observations of the steady head or pressure distribution and the transient mass concentration distribution of the contaminant, together with a few transmissivity observations. To obtain the distribution of velocity, the transmissivity is first determined by inverting the groundwater flow equation. The velocity components are then computed on the basis of Darcy's law, assuming the porosity and thickness of the aquifer are known. The computed velocity components are used for estimating unknown aquifer dispersivities in two-dimensional transient groundwater transport. In order to avoid the difficulty that often occurs in direct solution an integration-based method is presented. This method performs well in both noise free and relatively high noise level environments. In addition, a method to evaluate the additional parameters of dispersivity and velocity components is presented for the cases where the head or pressure distribution is not available. The equations for the methods are derived for cases in which the dispersivity varies with position, although the methods have not been tested for spatially varying dispersivities in the two-dimensional case.

Keywords: finite element method, integration method, parameter estimation, groundwater transport

Introduction

The threat of contaminants to groundwater supplies underscores the importance of understanding the processes of migration. The parameters of longitudinal and transverse dispersivity for problems controlled by hydrodynamic dispersion are desired from the inverse analysis. Dispersivity values obtained from tests on small samples can be viewed as representing a property of the medium but at a scale of insufficient size for general use in prediction of dispersion in the field. In comparison with the multitude of field hydraulic conductivity and transmissivity tests that have been conducted in geologic materials, only sparse dispersivity tests are reported. Numerical methods have been used to obtain parameters based on the dual measurements of head and contaminant concentration. Considerable work has been completed in this area. Strecker and Chu[1] developed an optimization procedure based on the United States Geological Survey–Method of Characteristics Model (USGS-MOC) for two-dimensional problems. The examples illustrated that the proposed algorithm could identify transmissivity and dispersivity accurately under ideal situations. Hafner and Schwan proposed a one-dimensional simulation scheme oriented along a flow path for steady-state groundwater flow.[2] They used a minimization procedure based on the steepest descent algorithm and discussed uniqueness and sensitivity of the solutions. Knopman and Voss analyzed the behavior of sensitivities, using a one-dimensional form of the advection-dispersion equation.[3] Their analysis showed that physical parameters can be determined more accurately at points in space and time with a high sensitivity to these parameters. The sensitivity to the dispersion coefficient is usually at least an order of magnitude less than that of velocity. The time and space interval over which an observation point is sensitive to a given parameter depends on the actual values of the parameters in the underlying physical system. Knopman and Voss[4] tested a nonlinear regression model[5] of solute transport in a one-dimensional analysis. The results illustrated that the regression models consistently converged to the correct parameters when the initial sets of parameter values substantially deviated from the correct parameters.

Umari et al. formulated a two-dimensional problem of transient groundwater transport from given observations as a general nonlinear problem using the concept of quasi-linearization.[6] The finite element method

Address reprint requests to Dr. Xiang at the Bureau of Economic Geology, The University of Texas at Austin, University Station, Box X, Austin, TX 78713–7508, USA.

Received 6 August 1991; revised 24 January 1992; accepted 14 February 1992

was used in conjunction with the finite difference method to discretize the governing differential equation (as constraints). The proposed algorithm was shown to be fast, stable, and accurate. Wagner and Gorelick demonstrated the utility of a nonlinear multiple-regression methodology for estimating parameters of contaminant transport.[7] The relative value of spatial data versus temporal data was investigated for estimation of velocity, dispersion coefficient, effective porosity, first-order decay rate, and zero-order production. The results showed that the use of spatial data gave estimates that were two to three times more reliable than those based on temporal data for all parameters except velocity.

However, all these previous studies describe procedures to determine an average value of dispersion coefficient representative of the region of interest. In addition, an indirect approach to determining the parameters required in flow and transport models, by adjusting the values of the parameters until the calculated solution matches observations, is often used. This is not the approach adopted here. Instead the following presents a finite element discretization of parameters, as well as the head and concentration, and then the finite element flow and transport equations are solved for the nodal values of parameters, taking the head and concentration distributions from observations. This is different from the normal use of the finite element method to solve for the head and concentration with given values of the parameters. In the case of sparse measurements, missing observations can be interpolated by an interpolation method, such as Kriging. The reduction of noise in observation and errors introduced in the interpolation is mentioned in another paper.[8]

In the following the differential equations for groundwater flow and transport are first introduced for forward solution. These equations are then cast in finite element form for direct inverse solution of problems with high dispersivity, and we use an integration method for problems with low dispersivity. To demonstrate the methods described in this paper, a one-dimensional example is finally presented.

Differential equations

Groundwater flow

Basic assumptions for the one- or two-dimensional problems of groundwater flow considered in the following are that the aquifer is horizontal, inhomogeneous from point to point, and continuous in the region. Only confined problems are considered where the transmissivity is directionally isotropic. The governing equation for a two-dimensional groundwater flow system under the above constraints was described by Huyakorn and Pinder[9] and can be written as

$$\frac{\partial}{\partial x_\alpha}\left(T_{\alpha\beta}\frac{\partial h}{\partial x_\alpha}\right) = \sum_{w=1}^{m_w} Q_w(t)\prod_\alpha \delta(x_\alpha - x_{\alpha w}) + S\frac{\partial h}{\partial t} \tag{1}$$

where α and β are the summation convention index (1 or 2) and x_1 and x_2 are coordinates, respectively, Π represents the product, m_w is the number of wells, and the solution of a two-dimensional equation must satisfy the following conditions:

$$h(x_1,x_2,0) = h_0(x_1,x_2) \qquad x_1,x_2 \text{ in } R \tag{2}$$

$$h(x_1,x_2,t) = h_I(x_1,x_2,t) \qquad x_1,x_2 \text{ in } R_I \tag{3}$$

$$T_{\alpha\beta}\frac{\partial h}{\partial x_\beta}(x_1,x_2,t)n_\alpha = h_{II}(x_1,x_2,t) \qquad x_1,x_2 \text{ in } R_{II} \tag{4}$$

where $h(x_1,x_2,t)$ is the head at point (x_1,x_2), $T_{\alpha\beta}$ is the transmissivity tensor at (x_1,x_2), S is storage coefficient, Q_w is flow rate at a well, R is the flow region, R_I and R_{II} are the boundaries of the aquifer, n_α is the component of the unit normal vector, h_0, h_I, h_{II} are specified functions, and x_{1w} and x_{2w} are the coordinate vectors of a well. Here, $\delta(x_\alpha)$ is the Dirac delta function.

Groundwater transport

A compact general equation for single mass concentration is the following[9]:

$$\frac{\partial}{\partial x_\alpha}\left(D_{\alpha\beta}\frac{\partial c}{\partial x_\beta}\right) - \frac{\partial}{\partial x_\alpha}(cV_{x_\alpha}) = \frac{\partial}{\partial t}k_r c \tag{5}$$

where k_r is the retardation coefficient, c is defined as contaminant concentration, n_p is porosity of the medium, V_{x_α} is velocity in the x_α direction, c_w is concentration at the well, $D_{\alpha\beta}$ is the hydrodynamic dispersion tensor, and

$$V_{x_k} = -\frac{T_{kk}}{bn_p}\frac{\partial h}{\partial x_k} \tag{6}$$

where $k = 1$ and 2 and k is a nonsummation index. In the absence of radioactive decay and desorption in a solution devoid of reactions, $k_r = 1$, and with point sources at x_{1w}, x_{2w} ($w = 1, 2, \ldots, m_w$) we have the following equation:

$$\frac{\partial}{\partial x_\alpha}\left(D_{\alpha\beta}\frac{\partial c}{\partial x_\beta}\right) - \frac{\partial}{\partial x_\alpha}(cV_\alpha) = \frac{1}{bn_p}\sum_{w=1}^{m_1} Q_w(t)c_w(t)\prod_\alpha \delta(x_\alpha - x_{\alpha w}) + \frac{\partial}{\partial t}k_r c \tag{7}$$

where b is thickness of the aquifer. The solution for concentration in equation (7) has to satisfy the following conditions:

$$c(x_1,x_2,0) = c_0(x_1,x_2) \qquad x_1,x_2 \text{ in } R \tag{8}$$

$$c(x_1,x_2,t) = c_I(x_1,x_2,t) \qquad x_1,x_2 \text{ in } R_{III} \tag{9}$$

$$-D_{\alpha\beta}\frac{\partial c}{\partial x_\beta}(x_1,x_2,t)n_\alpha + V_{x_\alpha}(x_1,x_2)n_\alpha = c_{II}(x_1,x_2,t) \qquad x_1,x_2 \text{ in } R_{IV} \tag{10}$$

where c_0, c_I, c_{II} are specified functions, n_α is defined as before, and R_{III} and R_{IV} are boundaries. According to Bear,[10] for an isotropic porous medium, $D_{\alpha\beta}$ can be expressed as

$$D_{\alpha\beta} = \alpha_T V \delta_{\alpha\beta} + (\alpha_L - \alpha_T)\frac{V_\alpha V_\beta}{V} \tag{11}$$

and

$$V = \sqrt{V_{x_1}^2 + V_{x_2}^2} \tag{12}$$

where α_L and α_T are longitudinal and transverse dispersivities of the porous medium, respectively.

Forward solution for contaminant transport

The finite element method is used for this problem, since it enables irregular boundary conditions to be readily accommodated. Therefore the continuous variables in this problem can be approximated as the following:

$$h(x_1,x_2,t) = \Phi_j(x_1,x_2)h_j(t) \tag{13}$$

$$T(x_1,x_2) = \phi_i(x_1,x_2)T_i \tag{14}$$

$$V_{x_\alpha}(x_1,x_2) = \phi_i(x_1,x_2)V_{x_{\alpha i}}(t) \qquad \alpha = 1,2 \tag{15}$$

$$c(x_1,x_2,t) = \Phi_j(x_1,x_2)c_j(t) \tag{16}$$

$$\alpha_L(x_1,x_2) = \phi_i(x_1,x_2)\alpha_{Li} \tag{17}$$

$$\alpha_T(x_1,x_2) = \phi_i(x_1,x_2)\alpha_{Ti} \tag{18}$$

where $\Phi_i(x_1,x_2)$ and $\phi_i(x_1,x_2)$ are shape functions applied to various variables and need not necessarily be the same, such as in the use of subparametric or superparametric elements.[11] In particular, we use $\Phi_i(x_1,x_2)$ for variables that involve the first derivative and $\phi_i(x_1,x_2)$ for variables that involve the second derivative in differential equations (1) and (7).

When head distributions at successive time steps are available, transmissivities can be obtained by solving equation (1) for the nonsteady problem, using equations (13) and (14).[8,12,13] Then the velocity components can be solved directly from equation (6) by using the computed transmissivities and observations of heads at any time level of interest.

Substituting equation (16) into equation (7) and using a weighting function $w_i = \phi_i$, then, we can transform the system of equations into the form,

$$\underline{A}\underline{c}^{n+1/2} - \underline{V}\underline{c}^{n+1/2} = \underline{q}_{wc} + \underline{q}_c - \underline{B}(\underline{c}^{n+1} - \underline{c}^n)/\Delta t \tag{19}$$

where $\underline{A}$ is a diffusive matrix, $\underline{q}_c$ is a vector of prescribed mass fluxes, $\underline{B}$ is a matrix representing element volumes, and

$$A_{ij} = \int_R D_{\alpha\beta}\frac{\partial\Phi_i}{\partial x_\alpha}\frac{\partial\Phi_j}{\partial x_\beta}\,dR \tag{20}$$

$$q_{ci} = \int_{R_{IV}} \Phi_i c_{II}\,dR_{IV} \tag{21}$$

$$q_{wci} = \begin{cases} Q_w c_w & \text{if well at node } (x_{1i},x_{2i}) \\ 0 & \text{if no well at node } (x_{1i},x_{2i}) \end{cases} \tag{22}$$

$$B_{ij} = \int_R \Phi_i\Phi_j\,dR \tag{23}$$

and $\underline{V}$ is a coefficient matrix representing the advective components in the transport equation as

$$V_{ij} = \int_R V_{x_\alpha}\frac{\partial\Phi_j}{\partial x_\alpha}\Phi_i\,dR \tag{24}$$

Therefore solution for the steady-state condition can be written as

$$(\underline{A} - \underline{V})\underline{c} = \underline{q}_t \tag{25}$$

where $\underline{q}_t = \underline{q}_{wc} + \underline{q}_c$. For nonsteady problems, finite differences in time can be used where the Crank-Nicolson method gives a simple and reliable way to evaluate the matrices as

$$\underline{F}_1\underline{c}^{n+1} = \underline{q}_t\underline{c}^{n+1} + \underline{q}_t\underline{c}^n - \underline{F}_2\underline{c}^n \tag{26}$$

where

$$\underline{F}_1 = \underline{A} - \underline{V} - \frac{2}{\Delta}\underline{B} \tag{27}$$

$$\underline{F}_2 = \underline{A} - \underline{V} + \frac{2}{\Delta}\underline{B} \tag{28}$$

and $\underline{q}_t^n$ and $\underline{q}_t^{n+1}$ are contaminant discharge vectors at time steps n and $n+1$, respectively. By evaluating the matrix relationship of equation (26) the contaminant concentration vector at time step $n+1$, $\underline{c}^{n+1}$ can be determined.

Direct solution for parameter estimation of dispersion coefficient

Assuming the transmissivity distribution to have been determined from equation (1) by the finite element method,[8,12,13] we can define the velocity components for a two-dimensional system by equation (15). Using discretized variables in equations (16)–(18) for equation (7) yields

$$\int_R \left(D_{\alpha\beta}\frac{\partial\Phi_i}{\partial x_\alpha}\frac{\partial\Phi_j}{\partial x_\beta} + V_{x_\alpha}\frac{\partial w_j}{\partial x_\alpha}\Phi_j\right) dR\, c_i - \int_{R_{IV}} c_{II} w_i\,dR_{IV} = -\frac{1}{bn_p}\sum_w Q_w - \int_R \frac{\partial c_i}{\partial t}\Phi_i w_j\,dR \tag{29}$$

Substituting equation (11) into equation (5) to reduce the number of unknown parameters and then into equation (29), and using the same weighting functions as shape functions defined in equation (16) together with the central difference method (Crank-Nicolson), enables this equation to be expressed in matrix form as

$$\underline{C}_T^{n+1/2}\underline{\alpha}_T + \underline{C}_L^{n+1/2}\underline{\alpha}_L = \underline{q}_c^{n+1/2} + \underline{q}_{wc}^{n+1/2} + \underline{v}_c^{n+1/2} - \frac{1}{\Delta t}\underline{B}(\underline{c}^{n+1} - \underline{c}^n) \tag{30}$$

where supscript $n + \frac{1}{2}$ represents the half time step and $\underline{c}^n$ and $\underline{c}^{n+1}$ are the mass concentration at time steps n and $n + 1$, respectively. Further applying of central differences to equation (30) yields

$$(\underline{C}_T^{n+1} + \underline{C}_T^n)\underline{\alpha}_T + (\underline{C}_L^{n+1} + \underline{C}_L^n)\underline{\alpha}_L = \underline{q}_c^{n+1} + \underline{q}_c^n + \underline{q}_{wc}^{n+1} + \underline{q}_{wc}^n + \underline{v}_c^{n+1} + \underline{v}_c^n - \frac{2}{\Delta t}\underline{B}(\underline{c}^{n+1} - \underline{c}^n) \quad (31)$$

where $\underline{C}_T^n$ is a matrix representing the distribution of concentration difference as a function of transverse dispersion coefficient, α_T, at time step n and $\underline{C}_L^n$ is a matrix representing the distribution of concentration difference as a function of longitudinal dispersion coefficient, α_L, at time step n. Now, $\underline{v}_c^n$ is a vector representing the sum of concentration distributions for the element where for a two-dimensional problem,

$$C_{Tjk}^n = c_i^n \sum_e \int_{R^e} \phi_k \left[\frac{V_{x_2}^2}{V}\frac{\partial\Phi_i}{\partial x_1}\frac{\partial w_j}{\partial x_1} - \frac{V_{x_1}V_{x_2}}{v}\left(\frac{\partial\Phi_i}{\partial x_2}\frac{\partial w_j}{\partial x_1} + \frac{\partial\Phi_i}{\partial x_1}\frac{\partial w_j}{\partial x_1}\right) + \frac{V_{x_1}^2}{V}\frac{\partial\Phi_i}{\partial x_2}\frac{\partial w_j}{\partial x_2}\right] dR^e \quad (32)$$

$$C_{Ljk}^n = c_i^n \sum_e \int_{R^e} \phi_k \left[\frac{V_{x_1}^2}{V}\frac{\partial\Phi_i}{\partial x_1}\frac{\partial w_j}{\partial x_1} + \frac{V_{x_1}V_{x_2}}{v}\left(\frac{\partial\Phi_i}{\partial x_2}\frac{\partial w_j}{\partial x_1} + \frac{\partial\Phi_i}{\partial x_1}\frac{\partial w_j}{\partial x_1}\right) + \frac{V_{x_2}^2}{V}\frac{\partial\Phi_i}{\partial x_2}\frac{\partial w_j}{\partial x_2}\right] dR^e \quad (33)$$

$$v_{cj}^n = c_i^n \sum_e \int_{R^e} \left(V_{x_1}\frac{\partial\phi_i}{\partial x_1}w_j + V_{x_2}\frac{\partial\phi_i}{\partial x_2}w_j\right) dR^e \quad (34)$$

where R^e is region of an element and Σ_e means the sum for all elements. To compute the elements C_{Tjk}^n, C_{Ljk}^n, and v_{cj}^n, a linear shape function ϕ and a constant function of Φ are used throughout this paper. The performance of both functions are evaluated by Xiang and Elsworth.[12] To solve equation (31) for the parameter vectors $\underline{\alpha}_L$ and $\underline{\alpha}_T$, equations written at two consecutive time levels $t = n + 1$ and $t = n + 2$ are needed as

$$(\underline{C}_T^{n+2} + \underline{C}_T^{n+1})\underline{\alpha}_T + (\underline{C}_L^{n+2} + \underline{C}_L^{n+1})\underline{\alpha}_L = \underline{q}_c^{n+2} + \underline{q}_c^{n+1} + \underline{q}_{wc}^{n+2} + \underline{q}_{wc}^{n+1} + \underline{v}_c^{n+2} + \underline{v}_c^{n+1} - \frac{2}{\Delta t}\underline{B}(\underline{c}^{n+2} - \underline{c}^{n+1}) \quad (35)$$

Equations (31) and (35) can be written in compact matrix form as

$$\begin{bmatrix} \underline{C}_T^{n+1} + \underline{C}_T^n & \underline{C}_L^{n+1} + \underline{C}_L^n \\ \underline{C}_T^{n+2} + \underline{C}_T^{n+1} & \underline{C}_L^{n+2} + \underline{C}_L^{n+1} \end{bmatrix} \begin{Bmatrix} \underline{\alpha}_T \\ \underline{\alpha}_L \end{Bmatrix} = \begin{Bmatrix} \underline{q}_t^{n+1} \\ \underline{q}_t^{n+2} \end{Bmatrix} \quad (36)$$

where $\underline{q}_t^{n+1}$ is the sum of right-hand terms in equation (31) and $\underline{q}_t^{n+2}$ is the same in equation (35).

After assembling the coefficients in equation (36), the least squares method can be used to reduce the residual error.[10] The parameter vectors, $\underline{\alpha}_T$ and $\underline{\alpha}_L$, can then be solved directly, provided adequate boundary conditions are defined.

Additional parameters

When the transmissivity cannot be obtained or the head distribution is not available, the velocity components cannot be determined from equation (6). This case makes inverse solution for the dispersion coefficients more difficult. However, if additional data sets defining the spatial distribution of contaminant concentration are available with time, and the dispersion coefficients are sufficiently large, these parameters, including velocity components, can be obtained from the inverse solution. Since the velocity components are not available, the dispersion coefficient cannot be obtained directly but can be defined indirectly through the components of the hydrodynamic dispersion coefficient. In this case there are five parameters that define each element for the two-dimensional problem (three components of hydrodynamic dispersion and two velocity components). Using a weighting function w and integrating equation (7) yields

$$\int_R \left[\frac{\partial}{\partial x_\alpha}\left(D_{\alpha\beta}\frac{\partial c}{\partial x_\beta}\right) - \frac{\partial}{\partial x_\alpha}(cV_{x_\alpha})\right] w\, dR = \frac{1}{bn_p}\int_R \left[\sum_{w=1}^{m_1} Q_w(t)c_w(t)\prod \delta(x_\alpha - x_{w\alpha}) + \frac{\partial c}{\partial t}\right] w\, dR \quad (37)$$

This equation can be further integrated by applying Green's theorem to obtain

$$\int_R \left[D_{\alpha\beta}\frac{\partial c}{\partial x_\alpha}\frac{\partial w}{\partial x_\beta} - \frac{\partial w}{\partial x_\alpha}(cV_{x_\alpha})\right] dR = \frac{1}{bn_p}\sum_{w=1}^{m_1} Q_w(t)c_w(t) + \int_R \frac{\partial c}{\partial t} w\, dR - \int_{R_{IV}} c_{II} w\, dR_{IV} \quad (38)$$

Using equation (15) and

$$D_{\alpha\beta} = D_{\alpha\beta k}\Phi_k \tag{39}$$

we can write equation (38) as

$$\underline{C}_{x_1}^{n+1/2}\underline{d}_1 + \underline{C}_{x_1x_2}^{n+1/2}\underline{d}_2 + \underline{C}_{x_2}^{n+1/2}\underline{d}_3 - \underline{C}_{ux_1}\underline{d}_4 - \underline{C}_{ux_2}\underline{d}_5 = \underline{q}_c^{n+1/2} + \underline{q}_{wc}^{n+1/2} - \frac{2}{\Delta t}\underline{B}(\underline{c}^{n+1} - \underline{c}^n) \tag{40}$$

By applying the central difference method to equation (41), and for four additional but similar equations written at successive time steps, a matrix solution can be obtained. Thus

$$\begin{bmatrix} \underline{C}_{11} & \underline{C}_{12} & \underline{C}_{13} & \underline{C}_{14} & \underline{C}_{15} \\ \underline{C}_{21} & \underline{C}_{22} & \underline{C}_{23} & \underline{C}_{24} & \underline{C}_{25} \\ \vdots & \vdots & \vdots & \vdots & \vdots \\ \underline{C}_{51} & \underline{C}_{52} & \underline{C}_{53} & \underline{C}_{54} & \underline{C}_{55} \end{bmatrix} \begin{Bmatrix} d_1 \\ d_2 \\ \vdots \\ d_5 \end{Bmatrix} = \begin{Bmatrix} f_1 \\ f_2 \\ \vdots \\ f_5 \end{Bmatrix} \tag{41}$$

where for $\xi = 1, 2, \ldots, 5$ we have

$$\underline{C}_{\xi 1} = \underline{C}_{x_1}^{n+1} - \underline{C}_{x_1}^{n} \tag{42}$$

$$\underline{C}_{\xi 2} = \underline{C}_{x_1x_2}^{n+1} - \underline{C}_{x_1x_2}^{n} \tag{43}$$

$$\underline{C}_{\xi 3} = \underline{C}_{x_2}^{n+1} - \underline{C}_{x_2}^{n} \tag{44}$$

$$\underline{C}_{\xi 4} = \underline{C}_{ux_1}^{n+1} - \underline{C}_{ux_1}^{n} \tag{45}$$

$$\underline{C}_{\xi 5} = \underline{C}_{ux_2}^{n+1} - \underline{C}_{ux_2}^{n} \tag{46}$$

and

$$C_{x_1jk}^{n} = \sum_e \int_R \Phi_k \frac{\partial\phi_i}{\partial x_1}\frac{\partial w_j}{\partial x_1} dR\, c_i^n \tag{47}$$

$$C_{x_2jk}^{n} = \sum_e \int_R \Phi_k \frac{\partial\phi_i}{\partial x_2}\frac{\partial w_j}{\partial x_2} dR\, c_i^n \tag{48}$$

$$C_{x_1x_2jk}^{n} = \sum_e \int_R \Phi_k \frac{\partial\phi_i}{\partial x_2}\frac{\partial w_j}{\partial x_1} + \frac{\partial\phi_i}{\partial x_1}\frac{\partial w_j}{\partial x_2} dR\, c_i^n \tag{49}$$

$$C_{ux_1jk}^{n} = \sum_e \int_R \Phi_k \phi_i \frac{\partial w_j}{\partial x_1} dR\, c_i^n \tag{50}$$

$$C_{ux_2jk}^{n} = \sum_e \int_R \Phi_k \phi_i \frac{\partial w_j}{\partial x_2} dR\, c_i^n \tag{51}$$

and n represents the time step; $\underline{d}_1$, $\underline{d}_2$, and $\underline{d}_3$ are hydrodynamic dispersion vectors $\underline{D}_{11}$, $\underline{D}_{12}$, and $\underline{D}_{22}$, respectively; $\underline{d}_4$ and $\underline{d}_5$ are velocity vectors V_{x_1} and V_{x_2}, respectively; and $\underline{f}_1$–$\underline{f}_5$ are the right-hand terms of equation (40).

A solution for the unknown parameters $\underline{D}_{11}$, $\underline{D}_{12}$, $\underline{D}_{22}$, $\underline{V}_{x_1}$, and $\underline{V}_{x_2}$ can be obtained from equation (41). With these parameters defined, the dispersion vectors, $\underline{\alpha}_T$ and $\underline{\alpha}_L$, can be determined directly by using velocity vectors $\underline{V}_{x_1}$ and $\underline{V}_{x_2}$ and equation (11).

When velocities are relatively small, dispersion plays an important role, enabling the dispersion coefficients to be obtained directly (see equation (11)). As the influence of dispersion becomes less apparent at higher flow velocities, the system of equations becomes less sensitive, making it difficult to determine dispersion coefficients. A solution can be obtained directly from equations (36) and (41). When more observations are available, the average and least squares methods can be used in this solution process to reduce the effect of noise on the result, as documented by Xiang and Elsworth.[8]

Figures 1 and *2* illustrate the effects of velocity and the dispersion coefficient, respectively, on the shape of the contaminant front at a time level of $t = 1.0$ sec. It is apparent that as velocity increases, the position of the front advances further forward but retains the same shape for the different velocities, as illustrated in *Figure 1*.

Figure 2 illustrates the relationship between the shape of the front and the magnitude of the dispersion coefficient. The front is very sharp when the dispersion coefficient is small, representing near plug flow, and flattens when the dispersion coefficient is large. From the characteristics illustrated in these two figures the time step between observations should be small for parameter estimation of dispersion coefficients in high-velocity transport to ensure accurate determination. However, when the dispersion coefficient is small, estimation is more difficult, and the proposed technique may not perform well. This suggests an alternative method outlined in the following.

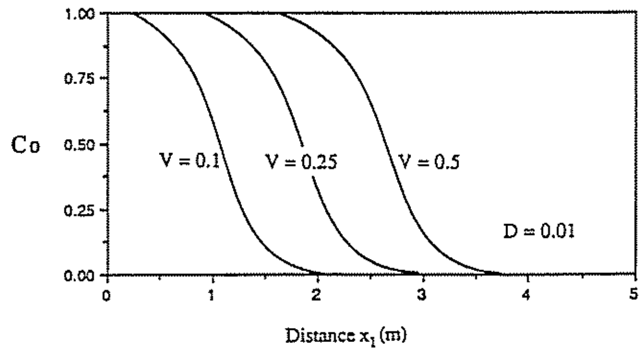

Figure 1. The relationship between relative concentration and distance (m) for different velocities (m sec^{-1})

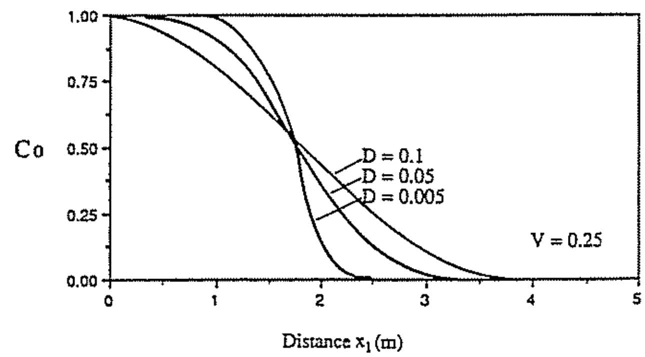

Figure 2. The relationship between relative concentration and distance (m) for different hydrodynamic dispersion coefficients (m^2 sec^{-1})

Integration method

In assembling the matrices $\underline{C}_L$ and $\underline{C}_T$ it is apparent that the concentration differences between adjacent nodes are the equivalent of head differences in the flow problem. If the difference in heads between adjacent nodes is zero, the inverse solution cannot be obtained from equations (36) and (41). Unlike the flow problem, however, where head differences may be maintained indefinitely, concentration differences will disappear with breakthrough of a contaminant front. As this occurs, concentration will remain near constant at all nodes, experiencing breakthrough for domains containing continuous sources. *Figure 3* illustrates, for a one-dimensional example, that when contaminant breakthrough occurs at node 4 ($x = 4$), all nodes behind the front exhibit the same concentration, suggesting that this kind of inverse problem cannot be solved. However, if a sufficiently long time period (i.e., long enough for the contaminant front to pass the region of interest) is considered and records of concentration for all times and all locations are available, the problem becomes determinate. The concentration histories at each location exhibit a unique breakthrough period, which is indexed to the dispersion coefficient in that element. The differences in contaminant volume between nodes for a time period $t = 5$ sec are shown as the shaded area in *Figure 4*. This illustrates that the differences in contaminant mass passing through nodes in a specified period can be obtained. For an adequately long period the differences in contaminant volume between nodes are constant. Consequently, it is this volume difference that should be used for inverse solution of dispersion coefficients, rather than concentration differences themselves. The only requirement of this method is that breakthrough occur at all nodes.

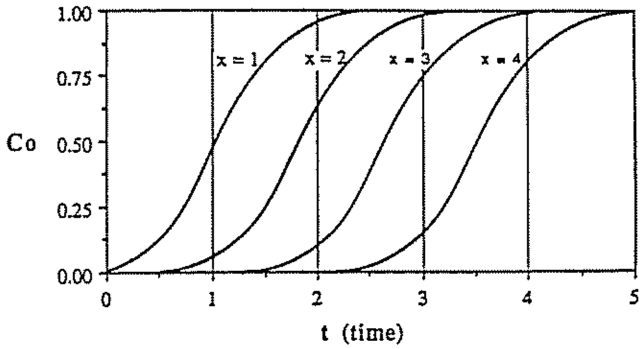

Figure 3. The relationship between relative concentration and time at different locations, where distance x (m) is used

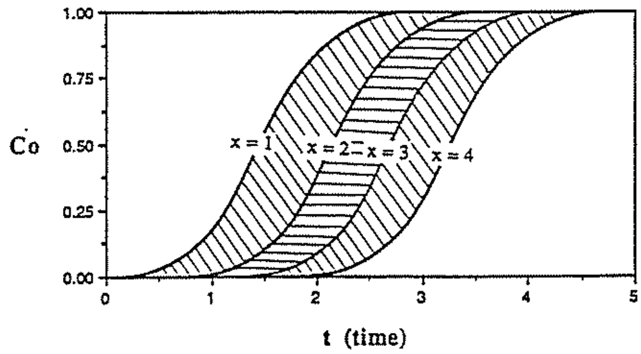

Figure 4. The relationship between relative concentration and time at different locations, where the shaded areas represent the volume difference between nodes and distance x (m) is used

An appropriate integration method must be used in this technique. The trapezoidal rule has been shown to perform best in this role[12] and will be used in the following. Integrating equation (7) yields

$$\int_{t_0}^{t_m}\left[\frac{\partial}{\partial x_\alpha}\left(D_{\alpha\beta}\frac{\partial c}{\partial x_\beta}\right)-\frac{\partial}{\partial x_\alpha}(cV_\alpha)\right]dt=\int_{t_0}^{t_m}\left[\frac{1}{bn_p}\sum_{w=1}^{m_1}Q_w c_w(t)\prod\delta(x_\alpha-x_{w\alpha})+\frac{\partial}{\partial t}c\right]dt \tag{52}$$

where t_0 is the initial time level and t_m is final time level. Based on the composite trapezoidal rule, equation (52) can be written as

$$\frac{1}{2}\left[\frac{\partial}{\partial x_\alpha}\left(D_{\alpha\beta}\frac{\partial c(t_0)}{\partial x_\beta}\right)+\frac{\partial}{\partial x_\alpha}\left(D_{\alpha\beta}\frac{\partial c(t_m)}{\partial x_\beta}\right)-\frac{\partial}{\partial x_\alpha}(c(t_0)V_{x_\alpha})-\frac{\partial}{\partial x_\alpha}(c(t_m)V_{x_\alpha})\right]+\sum_{k=1}^{m-1}\left[\frac{\partial}{\partial x_\alpha}\left(D_{\alpha\beta}\frac{\partial c(t_0)}{\partial x_\beta}\right)\right.$$
$$\left.-\frac{\partial}{\partial x_\alpha}(c(t_0)V_\alpha)\right]=\frac{1}{bn_p}\sum_{w=1}^{m_1}\left[\frac{1}{2}[Q_w(t_0)c_w(t_0)+Q_w(t_m)c_w(t_m)]+\sum_{k+1}^{m-1}Q_w(t_k)c_w(t_k)\right]\prod_\alpha\delta(x_\alpha-x_{w\alpha})+\frac{c(t_m)-c(t_0)}{\Delta t} \tag{53}$$

Similarly, the three components of hydrodynamic dispersion $D_{\alpha\beta}$ in the two-dimensional problem can be reduced into two unique dispersion coefficients through equation (11). Then, using the finite element method and substituting shape functions to discretize equation (53) yields

$$\left[\frac{1}{2}[\underline{C}_T(t_0)+\underline{C}_T(t_m)]+\sum_{k=1}^{m-1}\underline{C}_T(t_k)\right]\underline{\alpha}_T+\left[\frac{1}{2}[\underline{C}_L(t_0)+\underline{C}_L(t_m)]+\sum_{k=1}^{m-1}\underline{C}_L(t_k)\right]\underline{\alpha}_T$$
$$=\frac{1}{2}[\underline{q}_t(t_0)+\underline{q}_t(t_m)+\underline{v}_c(t_0)+\underline{v}_c(t_m)]+\sum_{k=1}^{m-1}[\underline{q}_t(t_k)+\underline{v}_c(t_k)]-\frac{1}{\Delta t}\underline{B}(\underline{c}_m-\underline{c}_0) \tag{54}$$

Since there are two unknown vectors, one further equation must be defined. Assuming concentration distribution to be available at a subsequent time level, then we can write an equation for the first m_2 observation sets as

$$\left[\frac{1}{2}[\underline{C}_T(t_0) + \underline{C}_T(t_{m_2})] + \sum_{k=1}^{m_2-1} \underline{C}_T(t_k)\right] \underline{\alpha}_T + \left[\frac{1}{2}[\underline{C}_L(t_0) + \underline{C}_L(t_{m_2})] + \sum_{k=1}^{m_2-1} \underline{C}_L(t_k)\right] \underline{\alpha}_T$$
$$= \frac{1}{2}[\underline{q}_t(t_0) + \underline{q}_t(t_m) + \underline{v}_c(t_0) + \underline{v}_c(t_{m_2})] + \sum_{k=1}^{m_2-1} [\underline{q}_t(t_k) + \underline{v}_c(t_k)] - \frac{1}{\Delta t} \underline{B}(\underline{c}_{m_2} - \underline{c}_0) \quad (55)$$

where m_2 is not the same as m.

Equations (54) and (55) can be written as

$$\begin{bmatrix} \underline{C}_{TT} \underline{C}_{TL} \\ \underline{C}_{LT} \underline{C}_{TT} \end{bmatrix} \begin{Bmatrix} \underline{\alpha}_T \\ \underline{\alpha}_L \end{Bmatrix} = \begin{Bmatrix} \underline{f}_t^n \\ \underline{f}_t^{n+1} \end{Bmatrix} \quad (56)$$

where

$$\underline{C}_{LL} = \frac{1}{2}[\underline{C}_L(t_0) + \underline{C}_L(t_m)] + \sum_{k=1}^{m-1} \underline{C}_L(t_k) \quad (57)$$

$$\underline{C}_{TL} = \frac{1}{2}[\underline{C}_T(t_0) + \underline{C}_T(t_m)] + \sum_{k=1}^{m-1} \underline{C}_T(t_k) \quad (58)$$

$$\underline{C}_{LT} = \frac{1}{2}[\underline{C}_L(t_0) + \underline{C}_L(t_{m_2})] + \sum_{k=1}^{m_2-1} \underline{C}_L(t_k) \quad (59)$$

$$\underline{C}_{TT} = \frac{1}{2}[\underline{C}_T(t_0) + \underline{C}_T(t_{m_2})] + \sum_{k=1}^{m_2-1} \underline{C}_T(t_k) \quad (60)$$

and f_t^n and f_t^{n+1} are the right-hand terms in (54) and (55), respectively. Solving equation (56) with appropriate boundary conditions enables the parameter vectors $\underline{\alpha}_L$ and $\underline{\alpha}_T$ to be obtained. In this method it is required that

$$t_m, t_{m_2} \geq t^* \quad (61)$$

where t^* is the time required for the contaminant front to break through within the entire region of interest.

Examples

A one-dimensional example is considered to demonstrate the proposed techniques. For inverse solution a constant finite element is used that returns superior results over those obtained by higher-order elements.[12] All the methods presented use the least squares method to reduce the residual error. The Gauss elimination method is used to solve equations (36), (41), and (56) for the desired parameters.

Problem and results

The problem of unidirectional transport in a one-dimensional aquifer is chosen. Boundary conditions of concentration at both ends are assumed known, but no measurements of dispersion coefficients are available. A total of 20 equal length elements are used to represent the system, with normalized concentrations of zero and unity applied at respective ends. Discharge quantities at both ends of the system are computed by forward estimation to obtain a true head distribution. A uniform velocity of $V = 1.0$ m sec^{-1} and uniform dispersion coefficient of $\alpha_L = 1.0$ m were used for the whole field. The concentration distributions computed at different time levels are illustrated in *Figure 5*.

Figure 5 shows that at early time the concentration profile within most elements is zero. As time advances, the concentration on the side behind the front increases, and the influence of dispersivity is quite apparent. Direct solution based on equation (36) is used in the inverse solution for dispersion coefficients. The distribution of dispersion coefficients computed by this method is illustrated in *Figure 6* for different moments in time. At early times the parameter distributions (as apparent in curves t = 1, 3, and 5 sec in *Figure 6*) are

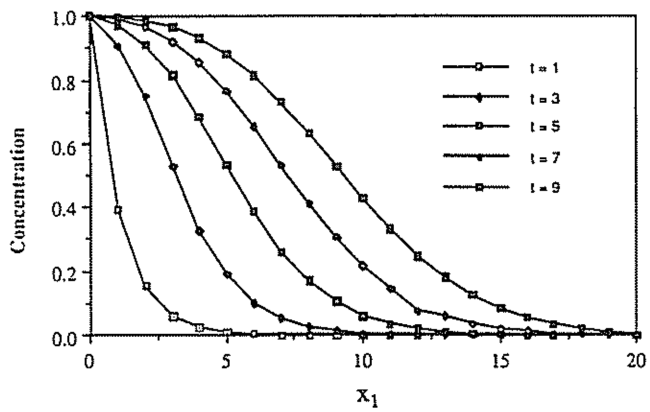

Figure 5. The relative concentration distribution along an aquifer for different times (sec)

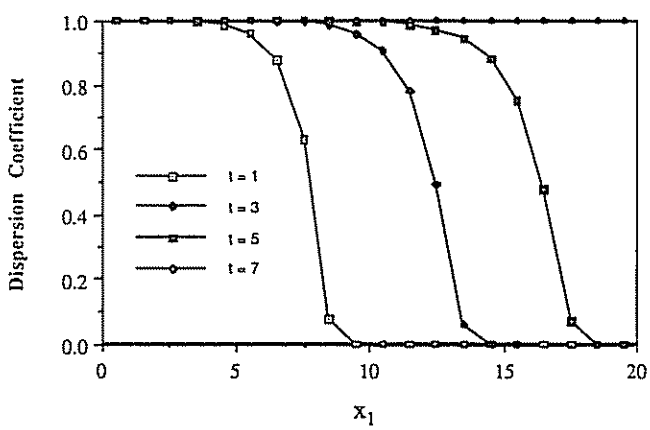

Figure 6. The distribution of the dispersion coefficient inverted along the aquifer for different times (sec)

incorrect, except where the concentration difference between nodes is nonzero.

However, as time advances, the parameter estimates improve. The curve representing $t = 7$ sec gives an exact solution for the dispersion coefficient in which no difference in concentration within the region is zero. At this stage the solution is optimal, since at future time steps, parameter estimation becomes indeterminate as the difference in concentrations approaches zero. *Figure 6* also illustrates that the average method mentioned previously does not perform satisfactorily, since correct solution is dependent on the time period. Before the contaminant front reaches the region of interest, the correct solution cannot be obtained. Only where dispersivity of the aquifer is very high and breakthrough occurs throughout the domain will this method yield good results.

Figure 7 illustrates the distribution of relative error associated with the inverted parameters for different individual variations of the real dispersion coefficient (D = 0.5, 1.0, 1.5, 2.0, and 2.5 m^2 sec^{-1}). The parameter sensitivity for different locations is illustrated in this figure, where coordinate x_1 represents the location of parameter variation. It is apparent that the error behind the front is lower than that ahead of the front and that the dispersion coefficient strongly affects the accuracy of the prediction behind the front. This suggests that because the sensitivity behind the front is higher, parameter determination will be more accurate for upstream locations than for locations ahead of the front.

Figure 8 illustrates the distribution of the sum of squares errors in evaluating the dispersion coefficient. It is apparent that when the dispersion coefficient is perturbed within the flow domain, the sum of squares errors in the parameter estimates on the side behind the front are little affected but ahead of the front the sensitivity is much greater. The relative magnitudes of the parameter also affect the accuracy, as is apparent in *Figure 8*. The greater the dispersion coefficient, the larger this effect, as is shown by the curve D = 2.5 m^2 sec^{-1} in *Figure 8*. This figure illustrates the effect of dispersivity variation on the estimated parameter distribution. From this figure it is apparent that better parameter estimation can be obtained in transport systems of uniform properties.

All errors shown in *Figures 7* and *8* illustrate that the error ahead of the front is larger than that behind the front. The local variation of dispersivity affects not only the parameters estimated at that location, but also the accuracy of the parameter distribution.

Additional parameter determination

In most practical problems the distribution of observed heads may not be available, but concentrations and appropriate boundary conditions may be determined. The method presented in the previous section can be applied to this case to obtain the distribution

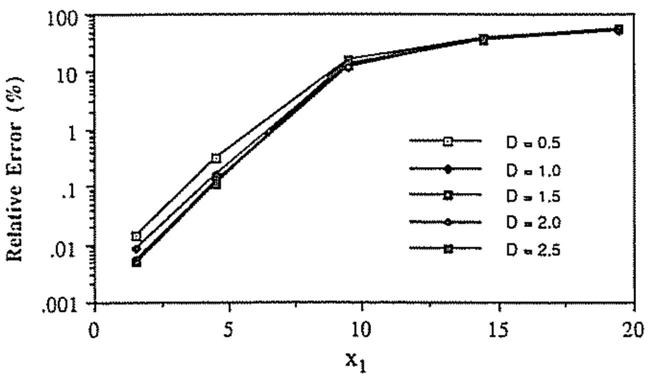

Figure 7. The distribution of relative error along an aquifer for the variation of real dispersion coefficients (m^2 sec^{-1}) at different locations

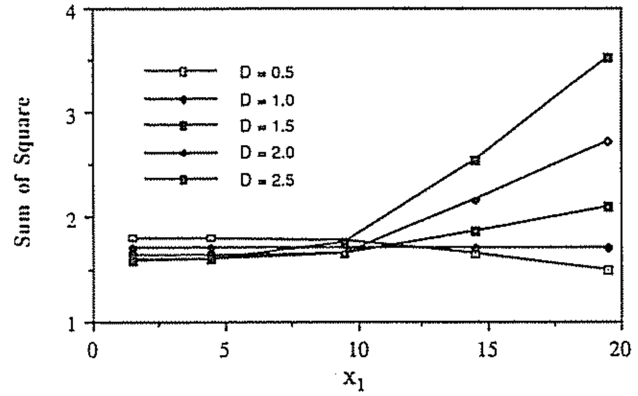

Figure 8. The distribution of the sum of squares error of inverted parameters along an aquifer for the variation of real dispersion coefficients (m^2 sec^{-1})

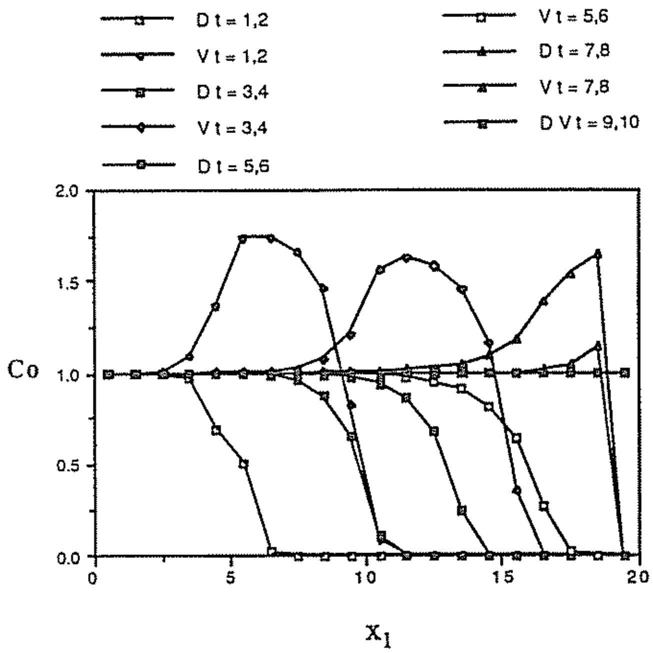

Figure 9. The distribution of parameters (dispersion coefficients and velocity) estimated by the expanded method along an aquifer for different times (sec)

Table 1. Sum of squares error of the dispersion coefficient for different noise levels

Noise level	Noise free	5%	10%	20%
Direct solution	0.54*E*-3	2.4914	4.655	14.085
Integration method	0.1861*E*-6	0.09536	0.4039	1.8444

of both dispersion coefficients and velocity components.

The same one-dimensional example as used previously is utilized, except that velocity remains as an unknown. Three distributions of concentration at successive time intervals are necessary to solve this problem. Under boundary conditions similar to the previous ones the distribution of estimated parameters is determined and illustrated in *Figure 9*. It is apparent that the distribution estimated at early time, similar to the case of estimation for dispersion coefficient alone, is poor but improves at late times. Furthermore, it is interesting to note that measurement of the dispersion coefficient on the boundary is not required for solution, since the coefficient matrix is no longer singular, provided the concentration gradient is sufficiently large. When the dispersion period is sufficiently long to enable three measurements of concentration to be made (three measurements for the one-dimensional problem and five measurements for the two-dimensional problem are needed), the parameters of velocity and dispersivity can be obtained with adequate precision, without prior knowledge of the porosity of the medium.

Results by integration method

All results reported previously illustrate that parameter estimation in transport problems depends primarily on dispersivity magnitudes and observation intervals. If the dispersion period is too short, parameters in most of the body cannot be adequately determined, and some numerical difficulty may also occur. To avoid these difficulties and successfully obtain parameters, the integration method can be used. If this method is applied to the previous example, the estimated parameters are almost exactly the same as the true solution. To compare this method with direct solution, several different noise levels can be considered. Noise may be randomly generated and added to the concentrations computed through forward solution. The sum of squares errors in the estimated parameters at different noise levels are illustrated in *Table 1*.

In comparing these values it is apparent that when the noise level is low, the sum of squares errors obtained by the integration method are two to three orders of magnitude less than those obtained by direct solution. As noise levels increase, this difference is reduced, but an order of magnitude difference still remains between the two methods. This suggests that the integration method performs better than direct solution in all circumstances.

Conclusions

Two finite element methods have been presented for parameter estimation of transport systems in the regions over which a concentration front has passed. A constant basis function element is used. The method has been used successfully in the estimation of both dispersion coefficients and velocity components. The following conclusions can be drawn from this analysis:

1. A direct algorithm that uses two subsequent measurements can be used for instances of high dispersivity where subsequent data sets are quite close in time. In the presence of random sampling noise the estimated parameters may be significantly affected.
2. An integration method that uses a full measurement profile yields improved accuracy. In addition, this method avoids numerical difficulties associated with many inverse solution techniques, and the effect of noise on the estimated parameters is largely reduced when compared with the direct algorithm.
3. Both direct and integration methods can be expanded to invert for extra parameters. When adequate concentration measurements are available, the head distribution is not required in the estimation of dispersivity and velocity components.
4. The constant basis function element ($\phi = 1$) performs very well in all instances. Because the assembled total coefficient matrix remains nonsingular, irrespective of the boundary conditions applied, the boundary condition of the dispersion coefficient need not be provided if contaminant flux is available. Consequently, the numerical solution for parameter estimation in transport systems can be readily applied to practical problems, since in situ measurement of the dispersion coefficient is difficult.
5. The equations for the methods are derived in cases for which the dispersivity is varying with position in a two-dimensional case, and it is considered that the methods would be applicable in such a case. However, the methods have not been tested for spatially varying dispersivities in a two-dimensional case.

Acknowledgments

The support of the National Abandoned Mine Land Reclamation Center is most gratefully acknowledged. We also wish to thank reviewers for their helpful comments and suggestions.

Nomenclature

$\underline{A}$	diffusive matrix
b	thickness of aquifer
$\underline{B}$	matrix representing element volumes
c, c_w	contaminant concentration and concentration at well, respectively
c_i, $\underline{c}^n$	contaminant concentration at note i

	and concentration vector at time step n, respectively
c_0, c_I, c_{II}	specified functions, concentration vector
$\underline{C}_T^n$, $\underline{C}_L^n$	matrix representing the distribution of concentration difference for α_T and α_L at time step n
$D_{\alpha\beta}$	components of hydrodynamic dispersion tensor
h, h_i	head and head at node i, respectively
h_0, h_I, h_{II}	specified functions
$\underline{h}$	vector of head
k_r	retardation coefficient
F_1, F_2	matrix formed by $\underline{A}$, $\underline{V}$, and $\underline{B}$
m, m_2	number of data sets
m_w	number of wells in region R
n	number of time steps
n_p	porosity of the porous medium
n_α	components in x_α direction of unit normal vector
$\underline{q}_i^n$	vector formed by right-hand vectors of equations (19), (31), and (35)
$\underline{q}_c^n$, $\underline{q}_{wc}$	discharge vector of wells for time step n
Q_w	discharge of well at note w
R	flow region
R_I, R_{II}	specified head boundary and discharge-prescribed boundary, respectively
R_{III}, R_{IV}	concentration boundary, contaminant inflow boundary condition, respectively
S	storativity of aquifer
Δt	time step
t_n	time and time level n
t^*	time required for contaminant front to break through within entire region of interest
$T_{\alpha\beta}$	transmissivity tensor and transmissivity at note i, respectively
V_{x_α}, $V_{x_{\alpha i}}$	velocity components and component at node i in x_α direction ($\alpha = 1$ or 2), respectively
$\underline{v}_c^n$	vector representing the sum of concentration distributions for the element at time n
$\underline{V}$	coefficient matrix representing the advective components
w	weighting function (if subscript, a well index)
x_α, $x_{\alpha w}$	coordinates and coordinates at wells
α_L, α_T, $\underline{\alpha}_L$, $\underline{\alpha}_T$	longitudinal and transverse dispersion coefficient and vectors, respectively
α, β	subscript for the summation index (1 or 2)
$\delta(x)$	Dirac delta function
Φ, ϕ	shape functions

References

1 Strecker, E. W. and Chu, W. Parameter identification of a ground-water contaminant transport model. *Ground Water* 1986, **24**, 56–62

2 Hafner, F. and Schwan, M. Simulation and parameter identification of mass transport in groundwater. *Ground Water* 1989, **26**, 631–637

3 Knopman, D. S. and Voss, C. I. Behavior of sensitivities in the one-dimensional advection-dispersion equation: Implications for parameter estimation and sampling design. *Water Resour. Res.* 1987, **23**, 253–272

4 Knopman, D. S. and Voss, C. I. Further comments on sensitivities, parameter estimation, and sampling design in one-dimensional analysis of solute transport in porous media. *Water Resour. Res.* 1988, **24**, 225–238

5 Van Genuchten, M. T. and Alves, W. J. Analytical solutions of the one-dimensional convective-dispersive solute transport equation. Tech. Bull. No. 1661, U.S. Dept. of Agric., Washington, DC, 1982

6 Umari, A., Willis, R., and Liu, P. L.-F. Identification of aquifer dispersivities in two-dimensional transient groundwater contaminant transport: An optimization approach. *Water Resour. Res.* 1979, **15**, 815–831

7 Wagner, B. J. and Gorelick, S. M. A statistical methodology for estimating transport parameters: Theory and applications to one-dimensional advective-dispersive systems. *Water Resour. Res.* 1986, **22**, 1303–1315

8 Xiang, J. and Elsworth, D. Parameter identification of nonsteady groundwater flow systems. *Adv. Water Resources* 1992, in press

9 Huyakorn, P. and Pinder, G. F. *Computational Methods in Subsurface Flow*. Academic, San Diego, CA, 1983

10 Bear, J. *Dynamics of Fluids in Porous Media*. Elsevier, New York, 1972

11 Desai, C. S. and Abel, J. F. *Introduction to the Finite Element Method: A Numerical Method for Engineering Analysis*. Van Nostrand Reinhold, New York, 1972, p. 97

12 Xiang, J. and Elsworth, D. Low-order finite elements for parameter identification in groundwater flow. *Appl. Math. Modelling* 1991, **15**, 256–266

13 Xiang, J. and Elsworth, D. A comparison of several optimization methods for inverse solution of groundwater flow systems. *Proceeding of the 5th Canadian and American Conference on Hydrogeology*, Calgary, Canada, September 1990